Heterozygous Variants of *CLPB* are a Cause of Severe Congenital Neutropenia

Tracking no: BLD-2021-010762R2

Julia Warren (Washington University, United States) Ryan Cupo (University of Pennsylvania, United States) Peeradol Wattanasirakul (Washington University, United States) David Spencer (Washington University School of Medicine, United States) Adam Locke (Regeneron Genetics Center, United States) Vahagn Makaryan (University of Washington, United States) Audrey Anna Bolyard (University of Washington, United States) Meredith Kelley (University of Washington, United States) Natalie Kingston (Washington University, United States) James Shorter (University of Pennsylvia, United States) Christine Bellanné-Chantelot (Pitié-Salpétrière Hospital, APHP, France) Jean Donadieu (Hopital Trousseau, France) David Dale (University of Washington School of Medicine, United States) Daniel Link (Washington University School of Medicine, United States)

Abstract:
Severe congenital neutropenia (SCN) is an inborn disorder of granulopoiesis. Approximately one-third of cases do not have a known genetic cause. Exome sequencing of 104 persons with congenital neutropenia identified heterozygous missense variants of *CLPB* (caseinolytic peptidase B) in 5 SCN cases, with 5 more cases identified through additional sequencing efforts or clinical sequencing. *CLPB* encodes an adenosine triphosphatase (ATPase) implicated in protein folding and mitochondrial function. Prior studies showed that biallelic mutations of *CLPB* are associated with a syndrome of 3-methylglutaconic aciduria, cataracts, neurologic disease, and variable neutropenia. However, 3-methylglutaconic aciduria was not observed and, other than neutropenia, these clinical features were uncommon in our series. Moreover, the *CLPB* variants are distinct, consisting of heterozygous variants that cluster near the ATP-binding pocket. Both genetic loss of *CLP*B and expression of *CLPB* variants results in impaired granulocytic differentiation of human hematopoietic progenitors and increased apoptosis. These CLPB variants associate with wildtype CLPB and inhibit its ATPase and disaggregase activity in a dominant-negative fashion. Finally, expression of *CLPB* variants is associated with impaired mitochondrial function but does not render cells more sensitive to endoplasmic reticulum stress. Together, these data show that heterozygous *CLPB* variants are a new and relatively common cause of congenital neutropenia and should be considered in the evaluation of patients with congenital neutropenia.

Conflict of interest: COI declared - see note

COI notes: All authors except JS declare no conflicts of interests. JS is a consultant for Dewpoint Therapeutics and Maze Therapeutics

Preprint server: No;

Author contributions and disclosures: Author Contributions DDCL and DCD conceived and jointly supervised the study. JTW, RRC, JS, DCD and DCL designed the experiments; JTW, RRC, PW, and NLK performed the experiments. DHS and AEL performed sequence alignment and variant annotation; JTW, PW and DCL analyzed SCNIR exome data and performed filtering. DCD, VM, MLK, and AAB provided patient samples and clinical information from the SCNIR; CBC and JD provided sequencing and clinical information from the French SCN Registry. JTW and DCL wrote the manuscript. All authors reviewed and contributed to the final version of the manuscript.

Non-author contributions and disclosures: No;

Agreement to Share Publication-Related Data and Data Sharing Statement: All data will be made available by email to the corresponding authors.

Clinical trial registration information (if any):

Title: Heterozygous Variants of *CLPB* are a Cause of Severe Congenital Neutropenia

Running Title: Heterozygous CLPB ATP-Binding Pocket Variants Cause SCN

Julia T. Warren[1], Ryan R. Cupo[2], Peeradol Wattanasirakul[3], David H. Spencer[3], Adam E. Locke[3], Vahagn Makaryan[4], Audrey A. Bolyard[4], Meredith L. Kelley[4], Natalie L. Kingston[5], James Shorter[2], Christine Bellanné-Chantelot[6], Jean Donadieu[7], David C. Dale[4], and Daniel C. Link[3]

[1]Division of Hematology-Oncology, Department of Pediatrics, Washington University School of Medicine, Saint Louis, MO, USA. [2]Department of Biochemistry and Biophysics, Pharmacology Graduate Group, Perelman School of Medicine at the University of Pennsylvania, Philadelphia, Pennsylvania, USA. [3]Division of Oncology, Department of Medicine, Washington University School of Medicine, Saint Louis, MO, USA. [4]Department of Medicine, University of Washington, Seattle, WA, USA. [5]Medical Scientist Training Program, Washington University School of Medicine, Saint Louis, MO, USA. [6]Département de génétique, Assistance Publique-Hôpitaux de Paris (AP-HP) Hôpital Pitié Salpêtrière, Sorbonne Université, Paris, France. [7]Sorbonne Université, Inserm, AP-HP, Registre français des neutropénies chroniques, Centre de référence des Neutrpénies chroniques, Hôpital Trousseau, Service Hémato oncologie Pédiatrique, F-75012 Paris, France.

Corresponding Authors:

Daniel C. Link, M.D.
Department of Medicine
660 South Euclid Avenue, Box 8007
St. Louis, MO 63110
Phone: (314) 362-8871
E-mail: danielclink@wustl.edu

David C. Dale, M.D.
Department of Medicine
University of Washington, Box 356422
Seattle, WA 98195
206-543-7215
dcdale@uw.edu

Word count (text and abstract): Text 4,336; Abstract 215; Figure/table count: 6 Figures /1 Table
Reference count: 39
Scientific category: Granulopoiesis

Key Points:

- Heterozygous variants in *CLPB*, clustered around the ATP-binding pocket, are a newly described and common cause of SCN
- ATP-binding pocket CLPB mutants act in a dominant-negative fashion to impair mitochondrial function and disrupt granulocytic differentiation

ABSTRACT

Severe congenital neutropenia (SCN) is an inborn disorder of granulopoiesis. Approximately one-third of cases do not have a known genetic cause. Exome sequencing of 104 persons with congenital neutropenia identified heterozygous missense variants of *CLPB* (caseinolytic peptidase B) in 5 SCN cases, with 5 more cases identified through additional sequencing efforts or clinical sequencing. *CLPB* encodes an adenosine triphosphatase (ATPase) implicated in protein folding and mitochondrial function. Prior studies showed that biallelic mutations of *CLPB* are associated with a syndrome of 3-methylglutaconic aciduria, cataracts, neurologic disease, and variable neutropenia. However, 3-methylglutaconic aciduria was not observed and, other than neutropenia, these clinical features were uncommon in our series. Moreover, the *CLPB* variants are distinct, consisting of heterozygous variants that cluster near the ATP-binding pocket. Both genetic loss of *CLP*B and expression of *CLPB* variants results in impaired granulocytic differentiation of human hematopoietic progenitors and increased apoptosis. These CLPB variants associate with wildtype CLPB and inhibit its ATPase and disaggregase activity in a dominant-negative fashion. Finally, expression of *CLPB* variants is associated with impaired mitochondrial function but does not render cells more sensitive to endoplasmic reticulum stress. Together, these data show that heterozygous *CLPB* variants are a new and relatively common cause of congenital neutropenia and should be considered in the evaluation of patients with congenital neutropenia.

INTRODUCTION

SCN is a rare bone marrow failure syndrome characterized by severe chronic neutropenia, an arrest of granulocytic differentiation at the promyelocyte or myelocyte stage, and a marked propensity to develop myeloid malignancies[1]. It has an estimated prevalence of 5 cases per million individuals. SCN demonstrates multiple modes of inheritance including autosomal recessive, autosomal dominant, X-linked, and sporadic patterns. The most frequently mutated gene in SCN is *ELANE*, which accounts for approximately 60% of SCN cases. ELANE mutations are also found in the majority of cases of cyclic neutropenia, a related disorder of granulopoiesis characterized by recurrent episodes of neutropenia with a 14-35 day periodicity. The genetic cause of approximately 30% of cases of SCN remains unknown.

Several groups recently reported that biallelic mutations of *CLPB* are associated with a syndrome characterized by 3-methylglutaconic aciduria (3-MGA), cataracts, neurologic disease, and neutropenia[2–5]. Neutrophils counts are variable, ranging from normal to chronic severe neutropenia. The *CLPB* mutations are distributed across the entire gene and include frequent nonsense or frameshift mutations[6], suggesting a loss-of-function mechanism of disease pathogenesis. CLPB encodes for caseinolytic peptidase B homolog, a member of the Clp/heat shock protein-100 family of ATPases[7]. Prokaryotic ClpB has been shown to catalyze protein unfolding and disaggregation in the setting of cellular stress[8–10]. This function is dependent on ATP hydrolysis and the formation of a hexameric ring through which substrate proteins are driven. Though the ATPase and disaggregase function of human CLPB has been confirmed[11,12] and it does appear to form higher order multimers[12], the exact structural basis for its function may differ as vertebrate CLPB only shares homology to the prokaryotic C-terminal ATPase domain and has a unique N-terminal region[2]. CLPB localizes to mitochondria[2,11,13,14], and it has been shown to regulate mitochondrial function[14].

Here, we report exome sequencing results of a large cohort of persons with congenital neutropenia. We identified heterozygous variants in *CLPB* that cluster in the ATP-binding pocket in 10 unrelated individuals. Expression of *CLPB* variants results in impaired granulocytic differentiation of human hematopoietic stem/progenitor cells (HSPCs) and is associated with reduced mitochondrial function. These data show that heterozygous ATP-binding pocket variants in *CLPB* are a new and relatively common cause of congenital neutropenia.

METHODS

Congenital neutropenia samples

Patients with congenital neutropenia were enrolled in the Severe Chronic Neutropenia International Registry (SCNIR) or the French chronic neutropenia registry, or identified through clinical sequencing. A total of 85 patients with congenital neutropenia were selected from the SCNIR based on prior *ELANE* genotyping, with the majority (70) having no *ELANE* mutation. Exome sequencing for the French registry cohort was performed on trios (proband-parents) after excluding the genes classically involved in SCN by targeted high throughput sequencing. All patients gave informed consent for these studies under protocols approved by local institutional review boards. DNA was extracted from blood, bone marrow or saliva samples.

Exome sequencing

Library preparation, sequencing, and data analysis details are provided in Supplementary Methods. Data were aligned to genome build GRCh38, and variants passing quality filters and present in the Exome Aggregation Consortium (ExAC) database[15] at a frequency <1% were identified. Mean gene expression was derived from data using 3 healthy donors with populations defined as previously reported[16]. The following criteria were used to identify

Downloaded from http://ashpublications.org/blood/article-pdf/doi/10.1182/blood.2021010762/1809413/blood.2021010762.pdf by WASHINGTON UNIVERSITY SCHOOL, Julia Warren on 11 June 2021

potentially pathogenic variants: 1) variants that altered amino acid sequence, including missense, nonsense, or splice site variants; 2) missense variants predicted to be deleterious based on a combined annotation dependent depletion (CADD) score ≥ 15; 3) variants with a frequency of < 0.0025 in the ExAC database[15]; and 4) variants in genes that are highly expressed in granulocyte precursors (TPM > 2). Variants of interest were further narrowed to those that had agreement between *in silico* predictions algorithms as further outlined in the supplemental methods. Copy number variation (CNV) analysis was performed with cnvkit[17] using default parameters to generate a reference copy number profile across all samples, followed by the 'batch' command for identification of CNVs in each sample.

Human HSPC Isolation and Culture

Human umbilical cord blood was obtained from the Saint Louis Cord Blood Bank. Mononuclear cells were enriched using Lymphoprep (StemCell Technologies). CD34+ cells were isolated using biotin anti-CD34 (Biolegend) antibody followed by enrichment with anti-biotin microbeads (Miltenyi). CD34+ cells were resuspended in StemSpan SFEMII with 100ng/mL of human stem cell factor (SCF), human thrombopoietin (TPO), and human Fms-like tyrosine kinase 3-ligand (FLT3-L) (PeproTech). Granulocytic differentiation was assessed by culturing cells in StemSpan SFEMII media with 3ng/mL of granulocyte-colony stimulating factor (G-CSF), 10ng/mL of SCF, and 10% fetal calf serum for 10-14 days. Colony forming unit-granulocyte (CFU-G) assays were performed using Methocult H4230 (StemCell Technologies) supplemented with G-CSF and SCF.

CRISPR/Cas9 knockout and Lentiviral Overexpression

A lentiviral vector was constructed based on the MND promoter for high expression in human hematopoietic cells[18,19]. Human *CLPB* encoding isoform 2 (the highest expressed isoform in

6

HSPCs and myeloid lineage cells) with a C-terminal hemagglutinin (HA) or c-Myc epitope tag was followed by an internal ribosomal entry site (IRES) linked to green fluorescent protein (GFP) or blue fluorescent protein (BFP). Following HSPC enrichment, CD34+ cells were transduced with lentivirus at a multiplicity of infection (MOI) of 15. To assess the degree of *CLPB* overexpression, RNA was isolated from day 7 cultures using a spin-column purification kit (Machery-Nagel) and cDNA was prepared using a reverse synthesis kit (Bio-rad). An exon-spanning probe was used to detect all isoforms of *CLPB*, and quantitative real-time PCR reactions was performed using a TaqMan Universal PCR Mastermix kit (Agilent Biosystems). For generation of knock-out cells using the clustered regularly interspaced short palindromic repeats (CRISPR)/Cas9 system, single guide RNA (sgRNA) were designed using the Broad Institute Genetic Pertubation Platform CRISPRko web-based tool (https://portals.broadinstitute.org/gpp/public/analysis-tools/sgrna-design). sgRNA were ordered from Synthego with 2'-O-metyl 3' phosphorothioate modifications in the capping nucleotides for increased stability. Recombinant Cas9 protein (IDT) was mixed with sgRNA and incubated at room temperature to generate ribonuclear protein complexes, followed by nucleofection in to HSPCs using the Neon system as previously described[20]. Insertion/deletion status was assessed by next generation sequencing (NGS) on the Illumina MiSeq platform, and analyzed using Crispresso2[21].

Flow cytometry

Cells were collected on the indicated day of culture and resuspended in phosphate-buffered saline (PBS) containing 0.1% bovine serum albumin (BSA) with human FC-block reagent (Trustain FcX, Biolegend) followed by incubation with antibodies on ice for 20 minutes. After washing, cells were resuspended in Sytox green for live/dead discrimination (Invitrogen). Granulocyte precursors were defined as: $CD33^+$, $CD14^-$, $CD11b^{+/-}$, $CD16^-$; and mature

neutrophils (PMN) were defined as: CD33+, CD14-, CD11b+, CD16+. Data was collected on an Attune NxT flow cytometer and analyzed using FlowJo v10. For apoptosis assays on primary human HSPCs, cells were placed in serum-free media for 16 hours then stained with neutrophil differentiation markers followed by fixation with BD Fix/Perm solution (BD Biosciences). Cells were stained with anti-cleaved caspase3 antibody (Biolegend). Apoptosis assays in the myeloid cell line MOLM-13 followed 24 hours of treatment with control dimethylsulfoxide (DMSO) or the glycosylation inhibiting drug tunicamycin (Sigma, St. Louis, MO) which was resuspended in DMSO and used at a final concentration of 1 uM. Cells were washed in EDTA-free media and resuspended in Annexin V-PE label according to the manufacturer's instructions or were fixed and stained for cleaved caspase-3 as above. For cell cycle analysis, following fixation cells were then stained with anti-Ki67 antibody, washed, and resuspended in FxCycle Violet (Invitrogen).

ATPase and Disaggregase Assays

Human CLPB protein containing amino acids 127-707, representing the ankyrin-rich repeat domains, ATPase domain, and C-terminal domain but lacking the N-terminal mitochondrial localization sequence and PARL-cleaved regulatory domains, was purified as previously described[11,22]. ATPase activity was assessed via detection of inorganic phosphate release using a malachite green detection assay (Expedeon) measured on a Tecan Infinite M1000 or Safire2 plate reader, as previously described[11,23]. Values represent background (time zero) subtracted from end-point colorimetric change. Luciferase disaggregation was performed using urea-denatured firefly luciferase, as previously described[11]. Detection of recovered luminescence was monitored using the above plate readers. For the mixing studies, WT CLPB was mixed either WT or variant CLPB at equimolar ratios for 10 minutes at 25°C (total protein concentration 4uM).

Confocal Imaging

8

Following lentiviral transduction, MOLM-13 cells were cytospun onto glass slides, fixed using the BD Perm/Fix reagent, permeabilized with 0.5% Triton X-100 (Sigma), and stained with antibodies to detect the C-terminal HA epitope tag on CLPB (Cell Signaling) or the mitochondrial marker TOM-20 (Cell Signaling) followed by incubation with secondary antibody (anti-rabbit Alexa Fluor 594 or anti-mouse Alexa Flour 647). Nuclei were counterstained with Sytox green, and slides were mounted in ProLong glass antifade (Thermo Fisher) then imaged on an LSM 700 confocal microscope (Carl Zeiss Microscopy) using a 63X objective. Images were processed using the Zeiss Zen software.

Mitochondrial Assays

MOLM-13 cells were lentivirally transduced as above using a BFP reporter plasmid, and sorted on BFP$^+$ cells. The mitochondrial stress test was performed according to manufacturer instructions and analyzed on a XF96e Seahorse (Agilent). Cells were then stained with Hoescht live cell nuclear stain (Sigma) and imaged on a Cytation5 analyzer (Biotek). Seahorse data were normalized to cell number and processed using the Wave software. To estimate mitochondrial mass, cells were washed with pre-warmed PBS and stained with Mitotracker green (Invitrogen) for 30 minutes in a 37°C incubator. Cells were then seeded on a CelTak coated 96-well black walled plate and imaged on a Cytation5 analyzer. To estimate mitochondrial membrane potential, cells were washed with pre-warmed PBS and adhered to a CelTak coated 96-well black walled plate using centrifugation then stained with the mitochondrial membrane potential sensitive dye tetramethyl rhodamine methylester (TMRM, Sigma) for 20 minutes in a 37°C incubator. Cells were imaged on a Cytation5 analyzer. Data were processed using the Gen software (Biotek) to create a cell-size mask, within which mean fluorescence intensity was calculated.

Statistical Analysis

Significance was determined using Prism v8.1.2 (GraphPad, San Diego, CA, USA). For single parameter analysis, unpaired t-test were used to assess statistical significance. For multiple parameter data, statistical significance was calculated using one-way or two-way analysis of variance (ANOVA). P values less than 0.05 were considered significant.

RESULTS

Heterozygous CLPB variants in congenital neutropenia

In an effort to identify novel genetic causes of SCN, we performed exome sequencing on 85 persons with congenital neutropenia recruited through the Severe Chronic Neutropenia International Registry (SCNIR); prior *ELANE* genotyping identified variants in 15 of 85 persons (**Table S1**). Using our filtering strategy defined in the methods section, we identified all known cases of *ELANE*-mutated congenital neutropenia and 8 cases of SCN with variants in established SCN-associated genes (**Fig. 1A**). In the remaining 62 cases of congenital neutropenia with no known genetic cause, we identified four unique heterozygous missense variants in *CLPB* in 5 persons with SCN. One additional SCN patient was initially identified through clinical sequencing and subsequently underwent exome sequencing confirming their heterozygous *CLPB* variant and the absence of other known SCN causative gene variants. Independently, exome sequencing was performed on 19 persons (and their parents) with chronic neutropenia without a known genetic cause enrolled in the French Chronic Neutropenia Registry (**Fig. 1B**). This identified one SCN patient with a *de novo* heterozygous *CLPB* variant. An additional three SCN cases with heterozygous *CLPB* variants were identified through targeted sequencing of 355 chronic neutropenia cases (**Fig. 1C**). Altogether, we identified 6 unique *CLPB* variants within 10 unrelated SCN patients (**Table 1**). Most of these variants were confirmed by Sanger sequencing (**Fig. S1**). For two of these patients, family studies were available and indicate *de novo* inheritance pattern (**Fig. 1D**). We also identified heterozygous *CLPB* variants in 2 cases of cyclic neutropenia in the SCNIR cohort, with a third case identified

10

in the French Neutropenia Registry; interestingly, all three cases carried the CLPB R628C variant (**Table S2**). No copy number alterations of *CLPB* were detected. Of note, we identified two additional *CLPB* variants that passed our filtering strategy (R327W and R603H); however, both were present in an asymptomatic parent, indicating they are likely benign and are therefore not included in Table 1.

Prior studies showed that biallelic variants of *CLPB* are associated with a syndrome (CLPB syndrome) characterized by 3-methylglutaconic aciduria (3-MGA), cataracts, neurologic disease, and variable neutropenia[2–5]. However, the variants seen in CLPB syndrome and *CLPB*-SCN are distinct. In patients with CLPB syndrome, the *CLPB* variants are always biallelic and are found scattered throughout the protein[6], with half of patients having at least one frame shift or nonsense variant (**Fig. 1E**). In contrast, the variants observed in our series are heterozygous, missense, and the localize to the C-terminal ATP-binding domain. We generated a structural model of human CLPB by threading the primary amino acid sequence onto that of *Thermus thermophilus* ClpB[24]. All 6 of the heterozygous CLPB-SCN variants are predicted to contribute to the ATP-binding pocket (**Fig. 1E**). Of note, these variants are in evolutionarily conserved residues and, by homology, most are predicted to be crucial residues for nucleotide binding and hydrolysis[24–26] (**Fig. S2**).

The clinical characteristics of the 10 patients with SCN carrying ATP-binding pocket *CLPB* variants is summarized in **Table 1.** All of the *CLPB*-SCN patients were diagnosed under the age of 5 and most received G-CSF therapy, with a median dose of 5.62 mcg/kg/day (a typical dose for SCN treatment). All demonstrated a myeloid maturation arrest and most had documented severe infections prior to G-CSF therapy. One patient developed a myeloid malignancy and is the only deceased patient from the cohort. In contrast to CLPB syndrome, in which 3-methylglutaconic aciduria is universal, none of the 5 patients in our series with available urine samples had 3-methylglutaconic aciduria[6]. Likewise, whereas cataracts and neurologic

11

abnormalities were present in more than 90% of cases of CLPB syndrome (very often co-occurring), they were uncommon in our *CLPB*-SCN cohort (2 non-overlapping patients each with cataracts or epilepsy, and 1 with developmental concerns). No case had more than one non-neutropenia CLPB syndrome feature. Of note, nearly 20% of patients with CLPB syndrome did not have neutropenia. The different clinical and molecular features of CLPB syndrome and *CLPB*-SCN suggest that these are distinct but related disorders with potentially unique mechanisms of disease pathogenesis.

Loss of CLPB results in impaired granulocytic differentiation

To assess the contribution of CLPB to granulopoiesis, we first used CRISPR-Cas9 gene editing to generate null mutations in *CLPB* in human cord blood CD34$^+$ hematopoietic stem/progenitor cells (HSPCs) (**Fig. S3A**). We were able to achieve greater than 80% editing efficiency, with a concordant decrease in protein expression (**Fig. S3B-D**). The gene-edited HSPCs were cultured in the presence of G-CSF and stem cell factor (SCF), and differentiation was assessed on day 14 by flow cytometry or by histomorphometry (**Fig. 2A-B**). Compared with HSPCs transduced with control sgRNA, significantly fewer mature neutrophils and an increase in granulocytic precursors were observed in cells transduced with two independent sgRNAs targeting CLPB. A significant decrease in CFU-G also was observed (**Fig. 2C**). Gene editing with the CRISPR-Cas9 system predominantly generates small insertion/deletions, some of which are in-frame and may yield functional, intact CLPB protein. Next-generation sequencing of cells from day 14 cultures showed a significant enrichment for non-targeted and in-frame *CLPB* sequences in neutrophils but not granulocytic precursors, consistent with a selective loss of *CLPB*-deficient cells during terminal granulocytic differentiation (**Fig. 2D**). Impaired granulocytic differentiation was at least in part due to increased apoptosis of early granulocytic precursors (**Fig. 2E**), with no change in cell cycle status observed (**Fig. 2F and Fig. S4**). Together, these data show that CLPB is required for normal granulocytic differentiation.

12

Expression of ATP-binding pocket CLPB variants results in impaired granulocytic differentiation

To assess the impact of heterozygous *CLPB* variants on granulopoiesis, we transduced cord blood CD34^{+} cells with lentivirus expressing each of the four CLPB variants from our SCNIR exome sequencing cohort (**Fig. 3A**). We included the likely benign, paternally inherited, non-ATP binding cleft R603H variant as a negative control. Of note, since CLPB expression was increased 4-10 fold compared to vector-alone controls (**Fig. 3B and Fig. S5)**, we included a wildtype CLPB lentiviral cohort to control for the effect of CLPB overexpression (**Fig. 3B**). A significant decrease in CFU-G was observed for the four *CLPB* variants that localize to the ATP-binding pocket (N496K, E557K, R561G, and R620C) but not the R603H variant (**Fig. 3C and 1E**). Fewer mature neutrophils and an increase in granulocytic precursors was present in cultures of HSPCs transduced with the ATP-binding pocket CLPB variants but not the R603H variant (**Fig. 3D-E**). Expression of ATP-binding pocket variants resulted in an increase in apoptosis of granulocytic precursors but no change in cell cycle status (**Fig. 3F-G**). Collectively, these data show that heterozygous ATP-binding pocket variants of *CLPB* cause impaired granulocyte differentiation.

CLPB heterozygous variants have impaired ATPase and disaggregase activity, and exert a dominant-negative effect on WT CLPB.

Human *CLPB* is an ATPase with potent disaggregase activity[11,12]. Biallelic *CLPB* variants that impair ATP cleavage also show impaired disaggregase activity, though there also appear to be ATPase-intact variants with impaired disaggregase activity that occurs through alternative mechanisms[11]. The heterozygous nature of our CLPB-SCN variants suggests a dominant negative effect on wildtype CLPB. To test this hypothesis, we performed mixing studies with recombinant WT and mutant CLPB proteins. As a control, we included the R408G CLPB variant that is found in biallelic CLPB syndrome in conjunction with a second CLPB

13

variant. Of note, parents with heterozygous R408G CLPB are asymptomatic[2,6], even though purified R408G protein has impaired ATPase activity[2]. We also included the likely benign variant, R603H. We show that all of the CLPB variants (except the R603H control) have impaired ATPase and disaggregase activity when tested in isolation (**Fig. 4A-B**). When mixed with WT CLPB, all of the heterozygous CLPB-SCN variants demonstrate greater than 50% reduction in both ATPase (reaching significance for E557K and R561G) and disaggregase activity (reaching significance for all CLPB-SCN variants) (**Fig. 4C-D**). In contrast, the R408G variant, while having reduced ATPase and disaggregase activity in isolation (**Fig. 4A-B**), did not suppress the activity of WT CLPB (**Fig. 4C-D**). As expected, the R603H variant had no effect. Together, these data suggest that heterozygous CLPB-SCN variants act in a dominant-negative fashion.

Expression of ATP-binding pocket CLPB variants results in impaired mitochondrial function

CLPB contains a mitochondrial localization sequence and has previously been shown to localize to the mitochondria in a human myeloid progenitor cell line, MOLM-13[14], and absence of CLPB causes impaired mitochondrial protein solubility[11]. Therefore, we hypothesized that CLPB-SCN heterozygous variants may affect granulocyte progenitors by impacting mitochondrial function. To test this hypothesis, we generated MOLM-13 cells expressing wildtype or mutant *CLPB*. We initially focused on CLPB N496K and R620C. Both wildtype and mutant *CLPB* localize to mitochondria (**Fig 5A**). CLPB mutant cells had impaired mitochondrial respiration, with significantly reduced basal and maximal respiratory capacity and a corresponding decrease in ATP production (**Fig. 5B-E**). A small but significant decrease in mitochondrial mass was observed in CLPB-N496K overexpressing cells, with a corresponding decrease in mitochondrial membrane potential, as measured using TMRM (**Fig. 5F-H**).

We next expanded our analysis to include other ATP-binding pocket variants from our heterozygous CLPB-SCN cohort (E557K, R561G, R561Q) and the two parentally inherited likely

14

benign variants (R327W and R603H). We also tested the R408G ATP-binding pocket variant, which is found in CLPB syndrome patients always in combination with nonsense or frameshift variants. As expected, the additionally tested ATP-binding pocket variants from our heterozygous-CLPB SCN cohort also demonstrated impaired mitochondrial function (**Fig 5I-K**). In contrast, one of the paternally inherited variants (R327W) did not. The other paternally inherited variant, R603H, displayed an intermediate phenotype. Interestingly, the R408G variant from the biallelic CLPB syndrome series did not show impaired mitochondrial function. The observed differences were not due impaired association of mutant CLPB with WT CLPB, as both R408G and our heterozygous CLPB-SCN variants were able to co-associate with WT CLPB (**Fig. S6**). Together, these data show that expression of ATP-binding pocket *CLPB*-SCN variants results in impaired mitochondrial respiration.

Expression of ATP-binding pocket CLPB variants does not render MOLM13 cells more sensitive to ER stress

During granulocytic differentiation, the massive expression of neutrophil elastase (encoded by *ELANE*), and other primary granule proteins, induces ER stress. Indeed, we and others reported that misfolded neutrophil elastase, through induction of ER stress, contributes to the pathogenesis of ELANE-mutated SCN[27-30]. ER stress can induce the unfolded protein response (UPR), ultimately resulting in apoptosis. Recent studies suggest that UPR-induced calcium efflux can enhance mitochondrial respiration, resulting in protection from ER-stress induced apoptosis[31,32]. Based on these observations, we hypothesized that the impaired mitochondrial respiration induced by mutant CLPB expression renders granulocytic precursors more sensitive to ER stress. To test this hypothesis, we induced ER stress in MOLM13 cells expressing CLPB N496K or R620C by treating with the glycosylation inhibiting drug tunicamycin. The magnitude of ER stress induced by tunicamycin, as measured by HSPA5 mRNA expression, was similar in control and *CLPB* mutant cells (**Fig. 6A**). In control (DMSO-

15

treated) cells, expression of N496K and R620C results in a small but significant increase in apoptosis as measured by cleaved Caspase 3 (**Fig. 6B**), with a trend to increased Annexin V cells surface expression (**Fig. 6C**). Although there was a significant increase in the total percentage of apoptotic cells in the N496K and R620C groups, all variants showed an equivalent fold-change increase in apoptosis relative to DMSO control (**Fig. 6D-E**). Thus, mutant *CLPB* expression does not render cells more sensitive to ER stress-induced apoptosis.

DISCUSSION

We identified 10 unrelated individuals with SCN and heterozygous ATP-binding pocket variants in *CLPB*. These patients present with isolated severe neutropenia with few, if any, of the non-hematopoietic features associated with bi-allelic *CLPB* loss, including 3-methylglutaconic aciduria. Expression of these *CLPB* variants in primary human HSPCs is sufficient to impair granulocytic differentiation. These observations suggest that heterozygous variants in *CLPB* that localize to the ATP-binding pocket are a new and relatively common cause of severe congenital neutropenia. Indeed, in the North American exome sequencing cohort, potentially pathogenic heterozygous *CLPB* mutations were identified in 5 of 70 (7.1%) of *ELANE*-wildtype SCN cases, making it the second most common cause of SCN behind *ELANE* mutations. We also establish the presence of potentially pathogenic heterozygous *CLPB* variants in the European population.

Not all heterozygous mutations in *CLPB* will be disease causing. Our data support a model whereby highly conserved mutations located within the ATP-binding pocket are predicted to be pathogenic. Our combination of sequencing and functional data allows us to classify the variants in 10 of these individuals as pathogenic or likely pathogenic according to American College of Medical Genetics criteria[33] (**Table S3**). We also identified two individuals with heterozygous variants in *CLPB* (R327W and R603H) that our functional data and inheritance patterns suggest are benign variants (**Table S4**). Of note, we also identified three unrelated

16

families with cyclic neutropenia carrying the *CLPB* variant R628C. Although not functionally validated, these data raise the possibility that this heterozygous *CLPB* variant may be a rare cause of cyclic neutropenia. Together, these observations indicate that genetic testing for *CLPB* should be included in the work-up of patients presenting with congenital neutropenia and importantly that heterozygous mutations in the ATP-binding pocket should be considered potentially pathogenic.

The mechanisms by which heterozygous ATP-binding pocket *CLPB* variants impair granulocytic differentiation are not clear. Genetic and biochemical evidence support a dominant-negative mechanism. Parents of patients with CLPB syndrome carrying heterozygous null *CLPB* mutations are asymptomatic[2-6]. Additionally, we show that ATP-binding pocket CLPB mutants co-immunoprecipitate with wildtype CLPB and inhibit the ATPase and disaggregase activity of wildtype CLPB in mixing studies. On the other hand, a simple dominant-negative mechanism does not account for all of the phenotypic differences between persons with heterozygous *CLPB* mutations and CLPB syndrome. In particular, 3-MGA was not detected in the urine of all evaluable CLPB-SCN cases (5 out of 10). In Pronicka's review of 31 patients with CLPB[6], urine 3-MGA was detected in 29 of 29 evaluable cases, whereas it was not detected in any of the 5 cases of CLPB-SCN where urine was available ($P < 0.0001$ compared to 0/5 CLPB-SCN cases, by Fisher's exact test). These observations suggest the possibility that, while the ATPase activity of CLPB is needed to maintain mitochondrial functions required for granulocytic differentiation, an (as yet undefined) ATPase-independent activity of CLPB helps maintain mitochondrial functions required to suppress 3-methylglutagonic production. In this model, the biallelic *CLPB* mutations in CLPB syndrome patients results in a loss (or partial loss) of all CLPB functions, resulting in both neutropenia, 3-methylglutagonic aciduria, and other nonhematopoietic phenotypes. In contrast, the heterozygous ATP-binding pocket mutations of CLPB found in SCN cases only impair the ATPase-dependent functions of CLPB, leading to severe neutropenia without 3-methylglutaconic aciduria. Further study is needed to test this

17

model, including careful examination for extra-hematopoietic phenotypes in all identified heterozygous CLPB-SCN cases. This will allow for clarification of whether ATP-binding pocket *CLPB* mutations define a unique clinical entity or contribute to a wider clinical spectrum of CLPB deficiency.

Our data suggest that expression of ATP-binding pocket CLPB mutants results in impaired mitochondrial function, and is similar to the phenotype of *CLPB* null cells[14]. Of note, our data show that mitochondrial respiration is significantly reduced in cells expressing mutant *CLPB* and this difference is not explained by the small (though significant) decrease in mitochondrial mass. This may be relevant, since during granulocytic differentiation there is a switch in energy metabolism from glycolysis to oxidative phosphorylation[34-36]. Whether impaired oxidative phosphorylation contributes to the impaired granulocytic differentiation induced by mutant CLPB will require further study. Although recent studies have suggested a link between ER stress and mitochondrial stress, our data suggest that the mitochondrial dysfunction induced by mutant CLPB expression does not appear to render cells more sensitive to ER stress. CLPB protein interacts with the mitochondrial proteins Optic Atrophy 1 (OPA1) and HAX1[11,14] and is required for HAX1 solubility[11]. Mutations of HAX1 are a rare cause of SCN[37] and OPA1 has been shown to regulate mitochondrial respiratory capacity through maintenance of mitochondrial cristae[38]. Whether heterozygous ATP-binding pocket mutations of *CLPB* alter interactions with OPA1 or HAX1 to disrupt mitochondrial function will require further study. Interestingly, although neutropenia is observed in some mitochondrial syndromes, such as Barth syndrome, it is not a common feature[39]. Thus, the specific mitochondrial defect may determine whether granulopoiesis is disrupted.

Establishing the link between SCN and heterozygous ATP-binding pocket mutations in *CLPB* will help guide the clinical management of these patients: they should be treated with G-CSF therapy as indicated and monitored closely for infection and development of myeloid

malignancy. Our findings also establish an important cell-intrinsic role for *CLPB* in normal human granulopoiesis. Future studies will be aimed at understanding the link between mitochondrial dysfunction and impaired granulocytic differentiation.

Acknowledgements

Author Contributions

DCL and DCD conceived and jointly supervised the study. JTW, RRC, JS, DCD and DCL designed the experiments; JTW, RRC, PW, and NLK performed the experiments. DHS and AEL performed sequence alignment and variant annotation; JTW, PW and DCL analyzed SCNIR exome data and performed filtering. DCD, VM, MLK, and AAB provided patient samples and clinical information from the SCNIR; CBC and JD provided sequencing and clinical information from the French SCN Registry. JTW and DCL wrote the manuscript. All authors reviewed and contributed to the final version of the manuscript.

Conflict of Interest Disclosures

All authors except JS declare no conflicts of interests. JS is a consultant for Dewpoint Therapeutics and Maze Therapeutics.

REFERENCES

1. Skokowa J, Dale DC, Touw IP, Zeidler C, Welte K. Severe congenital neutropenias. *Nat Rev Dis Primers*. 2017;3(1):nrdp201732.

2. Wortmann SB, Ziętkiewicz S, Kousi M, et al. CLPB mutations cause 3-methylglutaconic aciduria, progressive brain atrophy, intellectual disability, congenital neutropenia, cataracts, movement disorder. *American journal of human genetics*. 2015;96(2):245–257.

3. Saunders C, Smith L, Wibrand F, et al. CLPB variants associated with autosomal-recessive mitochondrial disorder with cataract, neutropenia, epilepsy, and methylglutaconic aciduria. *American journal of human genetics*. 2015;96(2):258–265.

4. Capo-Chichi J-M, Boissel S, Brustein E, et al. Disruption of CLPB is associated with congenital microcephaly, severe encephalopathy and 3-methylglutaconic aciduria. *Journal of Medical Genetics*. 2015;52(5):303–311.

5. Kiykim A, Garncarz W, Karakoc-Aydiner E, et al. Novel CLPB mutation in a patient with 3-methylglutaconic aciduria causing severe neurological involvement and congenital neutropenia. *Clinical immunology (Orlando, Fla.)*. 2016;165:1–3.

6. Pronicka E, Ropacka-Lesiak M, Trubicka J, et al. A scoring system predicting the clinical course of CLPB defect based on the foetal and neonatal presentation of 31 patients. *Journal of inherited metabolic disease*. 2017;40(6):853–860.

7. Snider J, Thibault G, Houry WA. The AAA+ superfamily of functionally diverse proteins. *Genome biology*. 2008;9(4):216.

8. Haslberger T, Zdanowicz A, Brand I, et al. Protein disaggregation by the AAA+ chaperone ClpB involves partial threading of looped polypeptide segments. *Nature structural & molecular biology*. 2008;15(6):641–650.

9. Deville C, Carroni M, Franke KB, et al. Structural pathway of regulated substrate transfer and threading through an Hsp100 disaggregase. *Science advances*. 2017;3(8):e1701726.

10. Rizo AN, Lin J, Gates SN, et al. Structural basis for substrate gripping and translocation by the ClpB AAA+ disaggregase. *Nature communications*. 2019;10(1):2393.

11. Cupo, RR, Shorter, J. Skd3 (human ClpB) is a potent mitochondrial protein disaggregase that is inactivated by 3-methylglutaconic aciduria-linked mutations. *eLife*. 2020;9:e55279.

12. Mroz, D, Wyszkowski, H, Szablewski, T, Zawieracz, K, Dutkiewicz, R, Bury, K, Wortmann, S, Wevers, R, Zietkiewicz, S. CLPB (caseinolytic peptidase B homolog), the first mitochondrial protein refoldase associated with human disease. *Biochem Biophys Acta Gen Subj*. 2020;1864(4):129512.

13. Yoshinaka T, Kosako H, Yoshizumi T, et al. Structural basis of mitochondrial scaffolds by prohibitin complexes: Insight into a role of the coiled-coil region. *Iscience*. 2019;19:1065–1078.

14. Chen X, Glytsou C, Zhou H, et al. Targeting Mitochondrial Structure Sensitizes Acute Myeloid Leukemia to Venetoclax Treatment. *Cancer Discov*. 2019;9(7):890–909.

15. Lek M, Karczewski KJ, Minikel EV, et al. Analysis of protein-coding genetic variation in 60,706 humans. *Nature*. 2016;536(7616):285–291.

16. Network CGAR, Ley TJ, Miller C, et al. Genomic and epigenomic landscapes of adult de novo acute myeloid leukemia. *The New England journal of medicine*. 2013;368(22):2059–2074.

17. Talevich E, Shain AH, Botton T, Bastian BC. CNVkit: Genome-Wide Copy Number Detection and Visualization from Targeted DNA Sequencing. *Plos Comput Biol*. 2016;12(4):e1004873.

18. Halene S, Wang L, Cooper RM, et al. Improved Expression in Hematopoietic and Lymphoid Cells in Mice After Transplantation of Bone Marrow Transduced With a Modified Retroviral Vector. *Blood*. 1999;94(10):3349–3357.

19. Robbins PB, Skelton DC, Yu XJ, et al. Consistent, persistent expression from modified retroviral vectors in murine hematopoietic stem cells. *Proceedings of the National Academy of Sciences of the United States of America*. 1998;95(17):10182–10187.

20. Brunetti L, Gundry MC, Kitano A, Nakada D, Goodell MA. Highly Efficient Gene Disruption of Murine and Human Hematopoietic Progenitor Cells by CRISPR/Cas9. *Journal of visualized experiments : JoVE*. 2018;(134):e57278–e57278.

21. Clement K, Rees H, Canver MC, et al. CRISPResso2 provides accurate and rapid genome editing sequence analysis. *Nature biotechnology*. 2019;37(3):224–226.

21

22. Cupo RR, Shorter J. Expression and Purification of Recombinant Skd3 (Human ClpB) Protein and Tobacco Etch Virus (TEV) Protease from *Escherichia coli. Bio Protoc*. 2020; 10(23):e3858.

23. DeSantis ME, Leung EH, Sweeny EA, Jackrel ME, Cushman-Nick M, Neuhaus-Follini A, Vashist S, Sochor MA, Knight MN, Shorter J. Operational plasticity enables hsp104 to disaggregate diverse amyloid and nonamyloid clients. *Cell*. 2012;141(4):778-793.

24. Lee S, Sowa ME, Watanabe Y, et al. The structure of ClpB: a molecular chaperone that rescues proteins from an aggregated state. *Cell*. 2003;115(2):229–240.

25. Zeymer C, Fischer S, Reinstein J. trans-Acting arginine residues in the AAA+ chaperone ClpB allosterically regulate the activity through inter- and intradomain communication. *Journal of Biological Chemistry*. 2014;289(47):32965–32976.

26. Wendler P, Ciniawsky S, Kock M, Kube S. Structure and function of the AAA+ nucleotide binding pocket. *Biochim Biophys Acta*. 2011;1823(1):2–14.

27. Grenda, D, Murakami, M, Ghatak, J, Xia, J, Boxer, L, Dale, D, Dinauer, M, Link, D. Mutations of the ELA2 gene found in patients with severe congenital neutropenia induce the unfolded protein response and cellular apoptosis. *Blood.* 2007;110(13): 4179 - 4187.

28. Nustede, R, Klimiankou, M, Klimenkova, O, Kuznetsova, I, Zeidler, C, Welte, K, Skokowa, J . ELANE mutant-specific activation of different UPR pathways in congenital neutropenia. *British J Haemat.* 2016;172(2):219 - 227.

29. Köllner, I, Sodeik, B, Schreek, S, Heyn, H, Neuhoff, N, Germeshausen, M, Zeidler, C, Krüger, M, Schlegelberger, B, Welte, K, Beger, CMutations in neutrophil elastase causing congenital neutropenia lead to cytoplasmic protein accumulation and induction of the unfolded protein response. *Blood*. 2006;108(2):493 - 500.

30. Nanua, S, Murakami, M, Xia, J, Grenda, D, Woloszynek, J, Strand, M, Link, D. Activation of the unfolded protein response is associated with impaired granulopoiesis in transgenic mice expressing mutant Elane. *Blood*. 2011;117(13):3539 - 3547.

31. Bravo, R, Vicencio, JM, Parra, V, Troncoso, R, Munoz, JP, Bui, M, Quiroga, C, Rodriguez, AE, Verdejo, HE, Ferreira, J, Iglewski, M, Chiong, M, Simmen, T, Zorzano, A, Hill, JA, Rothermel, BA, Szabadkai, G, Lavendero, S. Increased ER-mitochondrial coupling promotes mitochondrial respiration and bioenergetics during early phases of ER stress. *J Cell Sci*. 2011;124(Pt13):2143-52.

32. Knupp, J, Arvan, P, Chang, A. Increased mitochondrial respiration promotes purvival from endoplasmic reticulum stress. *Cell Death Differ*. 2019;26:487-501.

33. Richards, S, Aziz, N, Bale, S, Bick, D, Das, S, Fastier-Foster, J, Grody, W, Hegde, M, Lyon, E, Spector, E, Voelkerding, K, Rehm, H, on behalf of the ACMG Laboratory Quality Assurance Committee. Standards and Guidelines for the Interpretation of Sequence Variants: a Joint Consensus Recommendation of the American College of Medical Genetics and Genomics and the Association for Molecular Pathology. *Genetics in Medicine*. 2015;17: 405-423.

34. Vannini N, Girotra M, Naveiras O, et al. Specification of haematopoietic stem cell fate via modulation of mitochondrial activity. *Nat Commun*. 2016;7(1):13125.

35. Six E, Lagresle-Peyrou C, Susini S, et al. AK2 deficiency compromises the mitochondrial energy metabolism required for differentiation of human neutrophil and lymphoid lineages. *Cell Death Dis*. 2015;6(8):e1856–e1856.

36. Rice CM, Davies LC, Subleski JJ, et al. Tumour-elicited neutrophils engage mitochondrial metabolism to circumvent nutrient limitations and maintain immune suppression. *Nat Commun*. 2018;9(1):5099.

37. Klein C, Grudzien M, Appaswamy G, et al. HAX1 deficiency causes autosomal recessive severe congenital neutropenia (Kostmann disease). *Nature genetics*. 2007;39(1):86–92.

38. Mishra P, Carelli V, Manfredi G, Chan DC. Proteolytic Cleavage of Opa1 Stimulates Mitochondrial Inner Membrane Fusion and Couples Fusion to Oxidative Phosphorylation. *Cell Metab*. 2014;19(4):630–641.

39. Finsterer J. Hematological manifestations of primary mitochondrial disorders. *Acta haematologica*. 2007;118(2):88–98.

Table 1. Detailed Characteristics of Heterozygous SCN-CLPB Patients

Sample ID#	Protein p.	cDNA c.	VAF	gnomAD	Gender	Age at Diagnosis (Years)	Pre-G-CSF ANC	Median G-CSF dose (mcg/kg/day)	Bone Marrow Biopsy	Splenomegaly (Y/N)	AML/MDS (Y/N)	Infections	Neurological	Cataracts	Other	Urine 3-MGA**
Fr-0019	T388K	1163C>A	0.33	0	M	1.5	<0.5	5	Maturation arrest	No	No	Yes	Negative	Yes	Azoospermia neurinoma (age 41)	No
SCNIR-19	N496K	1488T>A	0.45	0	F	0.2	0.18	10.45	Maturation arrest	Yes	Yes	omphalitis at birth, otitis	Epilepsy	No	None	N/A
SCNIR-73	E557K	1669G>A	0.37	0	M	0	0.15	4.41	Maturation arrest	No	No	URI	Developmental delays	No	None	N/A
SCNIR-2	R561G	1681C>G	0.26	0	F	1.6	0.00	3.96	Maturation arrest	Yes	No	otitis, skin abscesses	Negative	No	None	No
SCNIR-2698*	R561Q	1682G>A	het	0	F	2.1	0.10	4.59	Maturation arrest	No	No	gangrenous appendicitis, sepsis; perianal abscess	Negative	No	None	N/A
Fr-0038	R561Q	1682G>A	0.48	0	F	0.5	0.45 - < 1	12.61	Maturation arrest	No	No	No	Negative	No	IUGR, GH deficiency, POF	No
Fr-1502	R561Q	1682G>A	0.52	0	F	0.25	0.1 - <1	11.92	Maturation arrest	No	No	Yes	Negative	Yes	None	N/A
Fr-0108	R561Q	1682G>A	0.47	0	M	2.5	0.7	No	Maturation arrest	No	No	Asperigillus	Epilepsy	No	Learning Difficulties	N/A
SCNIR-12	R620C	1858C>T	0.43	0	F	0.6	0.292	3.438	Maturation arrest	No	No	otitis, cellulitis, skin abscess, URI	Negative	No	None	No
SCNIR-29	R620C	1858C>T	0.47	0	F	0.2	0.00	3.45	Maturation arrest	No	No	None	Negative	No	None	No

SCNIR: Cases identified through the SCNIR North America registry; Fr: Cases identified through the French SCN registry
*Identified initially through clinical sequencing
**Urine organic acid testing specifically included quantitation of 3-MGA
URI: upper respiratory infection; UTI: urinary tract infection
IUGR: intrauterine growth restriction; GH: growth hormone; POF: premature ovarian failure
N/A: Not available

FIGURE LEGENDS

Figure 1. *CLPB* variants in SCN. Flow diagrams summarizing independent sequencing results from the SCNIR **(A)** and French SCN registry **(B-C)**. Cyclic: cyclic neutropenia. The number of cases carrying a specific variant is shown in parentheses. *One patient was identified initially through clinical sequencing, but subsequently enrolled in the SCNIR and underwent exome sequencing. **(D)** Mutational spectrum of *CLPB* as identified in this series (top) vs. previously reported biallelic variants (bottom). The overall domain architecture of human CLPB is shown and includes the mitochondrial localization sequence (MLS); ankyrin-rich repeats (ANK); ATPase domain, and C-terminal domain (CTD). **(E)** CLPB protein structure model based on data from the crystal structure of *Thermus Thermophilus* CLPB (PDB ID: 1qvr). Side chains are shown for the 5 mutated residues found in 10 patients which cluster around the ATP-binding pocket. **(F)** Pedigrees for 2 *de novo* cases with available family studies. Parental and patient variant status was confirmed using Sanger sequencing. "WT": wild-type, indicating that the relevant *CLPB* variant was not present. Parentage for cases Fr-0019, Fr-0038 and Fr-1408 were confirmed using short tandem repeat analysis.

Figure 2. *CLPB* deficient HSPCs have impaired granulocytic differentiation. Human cord blood CD34$^+$ cells were nucleofected with guide RNA targeting CLPB (CLPB-g1 or CLPB-g3), or a control guide RNA targeting the intron of *AAVS1* (as a gene editing control) complexed together with recombinant Cas9 protein. Edited CD34$^+$ cells were cultured for 7-14 days in media containing G-CSF and stem cell factor. **(A)** Representative flow plots showing gating strategy to identify CD11b$^+$, CD16$^+$ mature neutrophils (PMN) or CD11b$^{+/-}$ CD16$^-$ granulocytic precursors; data are gated on CD14$^-$ cells to remove monocytes. Data are quantified in the right panel. **(B)** Representative hematolylin/eosin stained cytospin preparations of cells on day 14 of culture; original magnification 63X. Data are quantified in the right panel. **(C)** Shown are the number of colony-forming units-granulocyte (CFU-G) per 2,000 gene-edited CD34$^+$ cells. **(D)**

Fold change (from day 0) in edited (for *CLPB*, edited out-of-frame) or unedited cells (for *CLPB*, unedited plus edited in-frame) in PMNs or granulocytic precursors sorted on day 14. **(E)** Percentage of caspase-3$^+$ granulocytic precursors on day 7 of culture. **(F)** Cells were cultured for 7 days and cell cycle was assessed by flow cytometry. Data represent 3-5 independent experiments. *p<0.05, **p<0.01, ***p<0.005. Statistical significance was determined using repeated measures one-way ANOVA.

Figure 3. Expression of ATP-binding pocket *CLPB* mutants impairs granulocytic differentiation. Cord blood CD34$^+$ cells were transduced with lentivirus expressing the indicated *CLPB* cDNA (or empty vector control). GFP$^+$ cells were sorted at 48 hours, then seeded into media containing G-CSF and stem factor or methylcellulose containing G-CSF. **(A)** Lentiviral vector. LTR; long terminal repeat; HA; hemagglutinin epitope tag; IRES: internal ribosomal entry site; GFP: green fluorescent protein; WPRE: woodchuck promoter responsive element. **(B)** RNA expression of *CLPB* relative to β-actin mRNA. **(C)** CFU-G per 2,000 GFP$^+$ CD34$^+$ cells. **(D-E)** The percentage of mature neutrophils (**D**) and granulocytic precursors (**E**) on day 14 of culture is shown; data are gated on CD14$^-$ cells to exclude monocytes. **(F)** Percentage of caspase-3$^+$ granulocytic precursors on day 7 of culture. **(G)** Cells were cultured for 7 days and cell cycle was assessed by flow cytometry. Data represent 3-5 independent experiments. *p<0.05,**p<0.01,***p<0.005. Statistical significance was determined using repeated measures one-way ANOVA.

Figure 4. CLPB mutants show impaired ATPase and disaggregase activity, and exhibit a dominant negative effect on WT CLPB. Purified CLPB protein was used to measure (**A**) ATPase activity of the indicated CLPB variants tested in isolation; (**B**) Disaggregase activity of the indicated CLPB variants tested in isolation; (**C**) ATPase activity of WT CLPB when mixed 1:1 with WT CLPB or CLPB variants; and (**D**) Disaggregase activity of WT CLPB when mixed
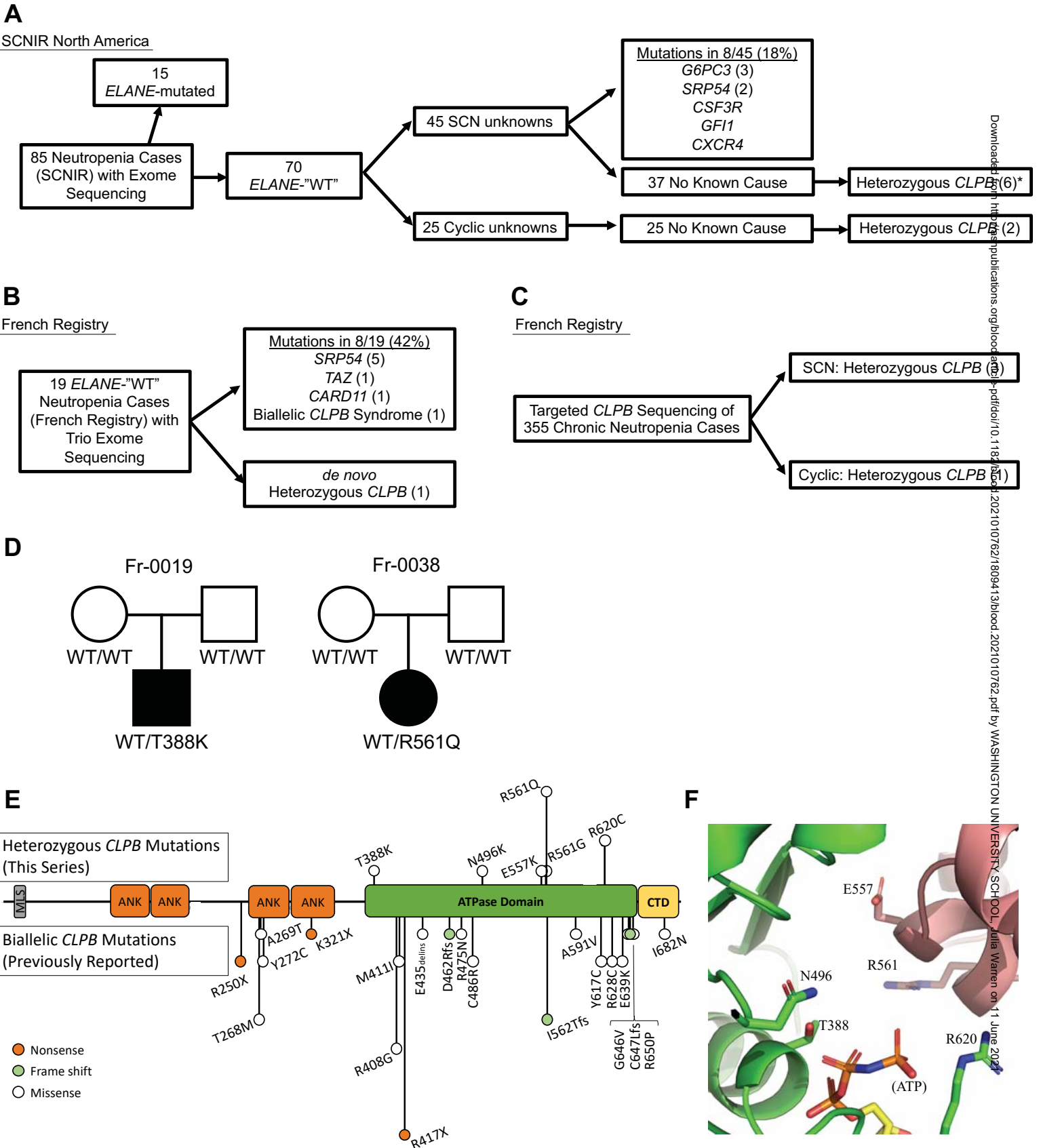
1:1 with WT CLPB or CLPB variants. For (**C-D**), the dashed line represents 50% of WT CLPB activity. Data represent 3 independent experiments. For (**A-B**), comparison was made to WT CLPB activity. For (**C-D**), comparison was made to values representing 50% of WT activity. *$p<0.05$, ** $p<0.01$, ***$p<0.001$, ****$p<0.0001$. Statistical significance was determined using one-way ANOVA.

Figure 5. Expression of CLPB mutants impairs mitochondrial respiration without affecting membrane potential. MOLM-13 cells were transduced with a lentiviral vector expressing *WT CLPB, CLPB-N496K,* or *CLPB-R620C*. **(A)** Representative photomicrographs of cells stained with anti-HA antibody to detect CLPB (red) and anti-TOM20 (yellow) to label mitochondria. Nuclei were counterstained with Sytox (blue); original magnification 63X. **(B-E)** The mitochondrial stress test was performed using the Seahorse XF96e analyzer. **(B)** Representative graph showing the oxygen consumption rate (OCR) at baseline and after treatment with the ATP synthase inhibitor oligomycin (OM) and then the uncoupling agent carbonyl cyanide-4 phenylhydrazone (FCCP). Parameters of mitochondrial respiration include **(C)** Basal respiration; **(D)** Maximal respiration and **(E)** total ATP production. **(F-H)** Cells were labeled with tetramethylrhodamine (TMRM) or mitotracker green (MG). **(F)** Mitotracker green signal normalized to empty vector control. **(G)** TMRM signal normalized to empty vector control. **(H)** Ratio of TMRM signal to mitotracker green signal is shown. Mitochondrial respiration parameters for additional *CLPB* variants: **(I)** Basal respiration; **(J)** Maximal respiration and **(K)** total ATP production. *$p<0.05$,**$p<0.01$. Statistical significance was determined using repeated measures one-way ANOVA.
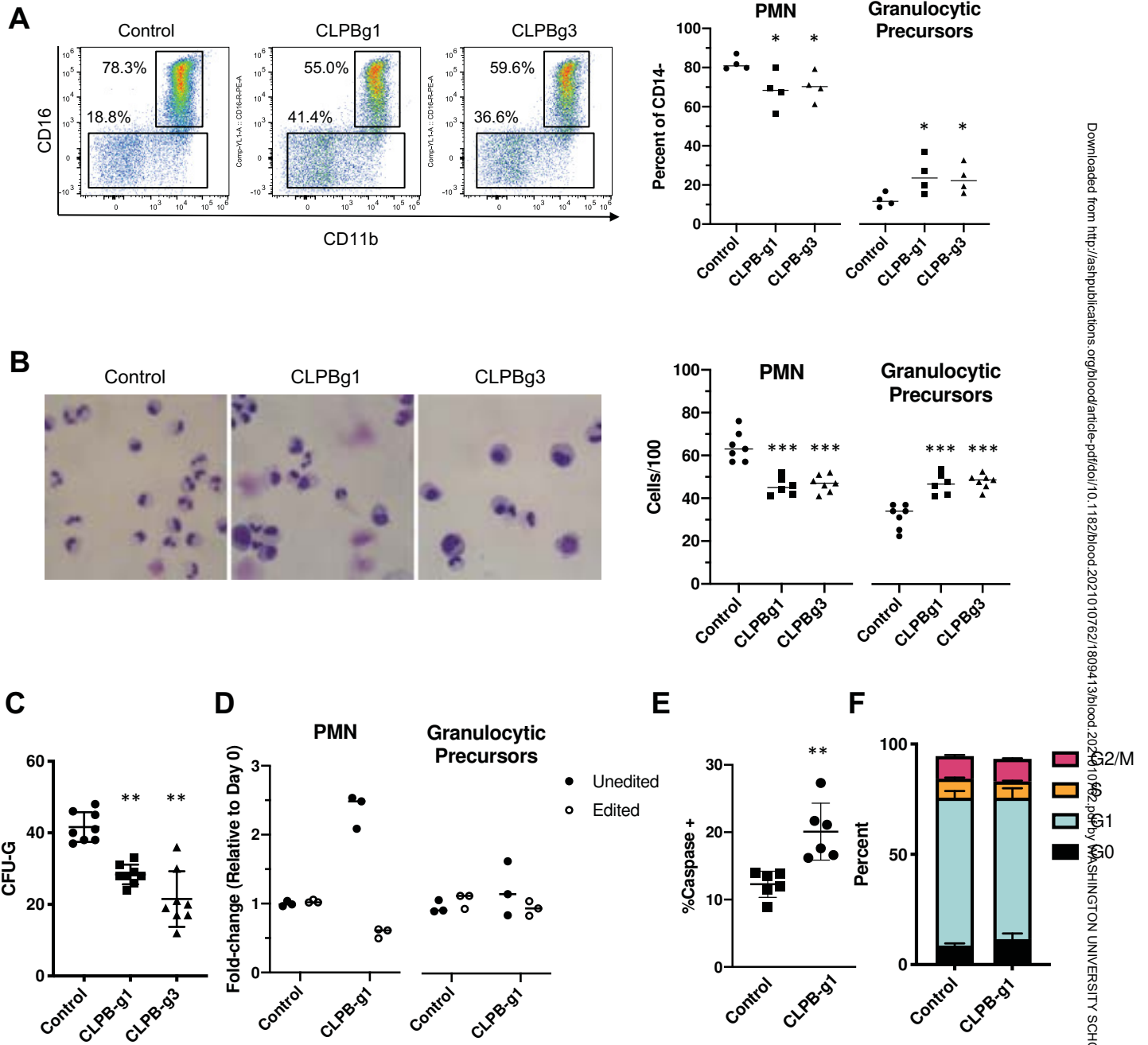
Figure 6. Induction of UPR Does Not Cause Increased Fold-change in Apoptosis in CLPB Variant-Expressing Myeloid Cells. The myeloid cell line MOLM-13 was transduced with CLPB variants or empty vector control and cells were sorted based on GFP-positivity. Cells were

treated with DMSO (D) or the glycosylation-inhibitor tunicamycin (TM) for 24 hours. **(A)** Induction of the UPR was confirmed by assessing expression of HSPA5 by qPCR. The percentage of cleaved caspase-3+ **(B)** or Annexin V+ **(C)** cells was assessed by flow cytometry. Fold-change representation of cleaved caspase-3+ **(D)** or the Annexin V+ **(E)** cells expressed as the ratio of tunicamycin divided by DMSO within each sample. Data represent 3 independent experiments. *p<0.05,**p<0.01,***p<0.001. Statistical significance was determined using repeated measures one-way ANOVA.
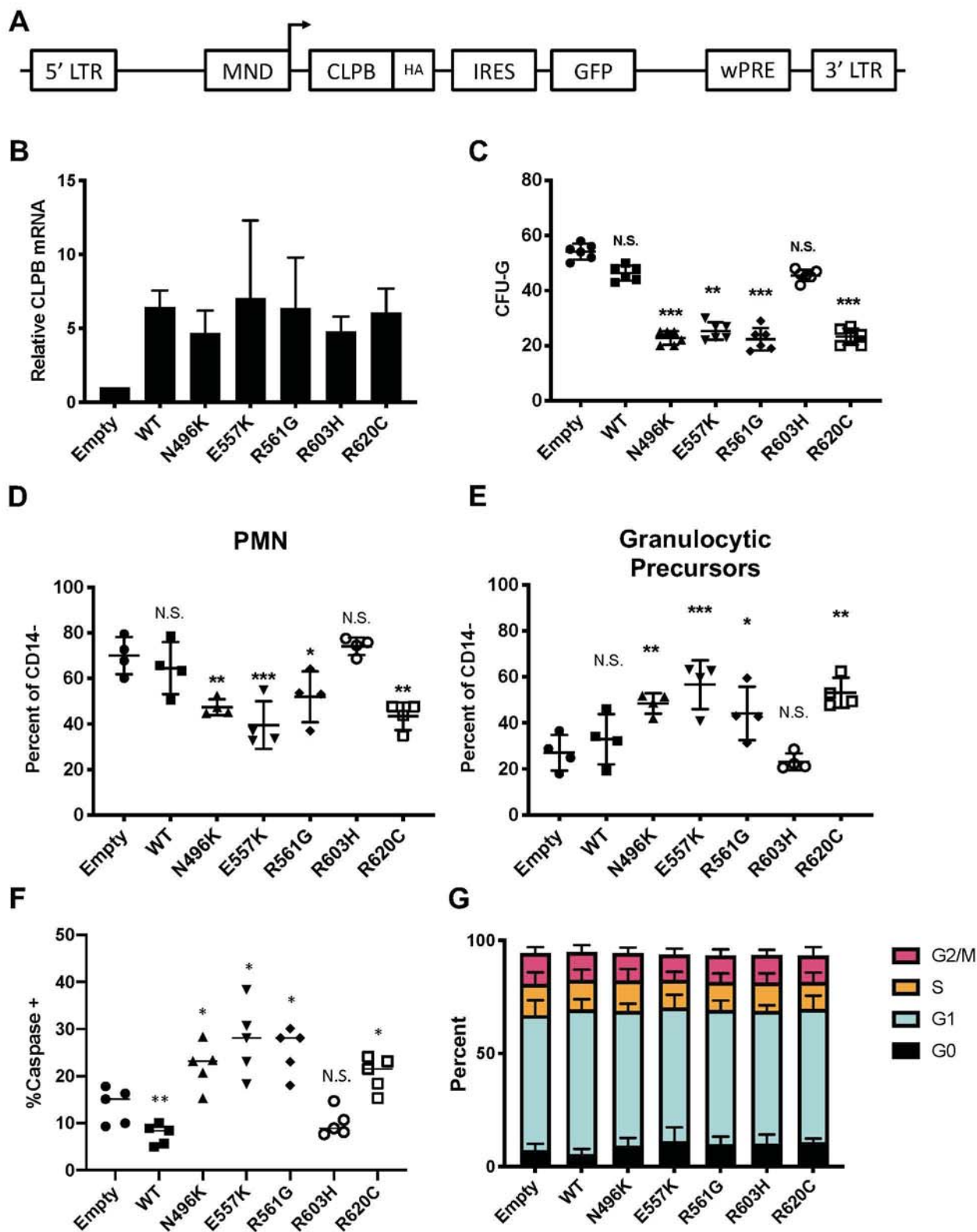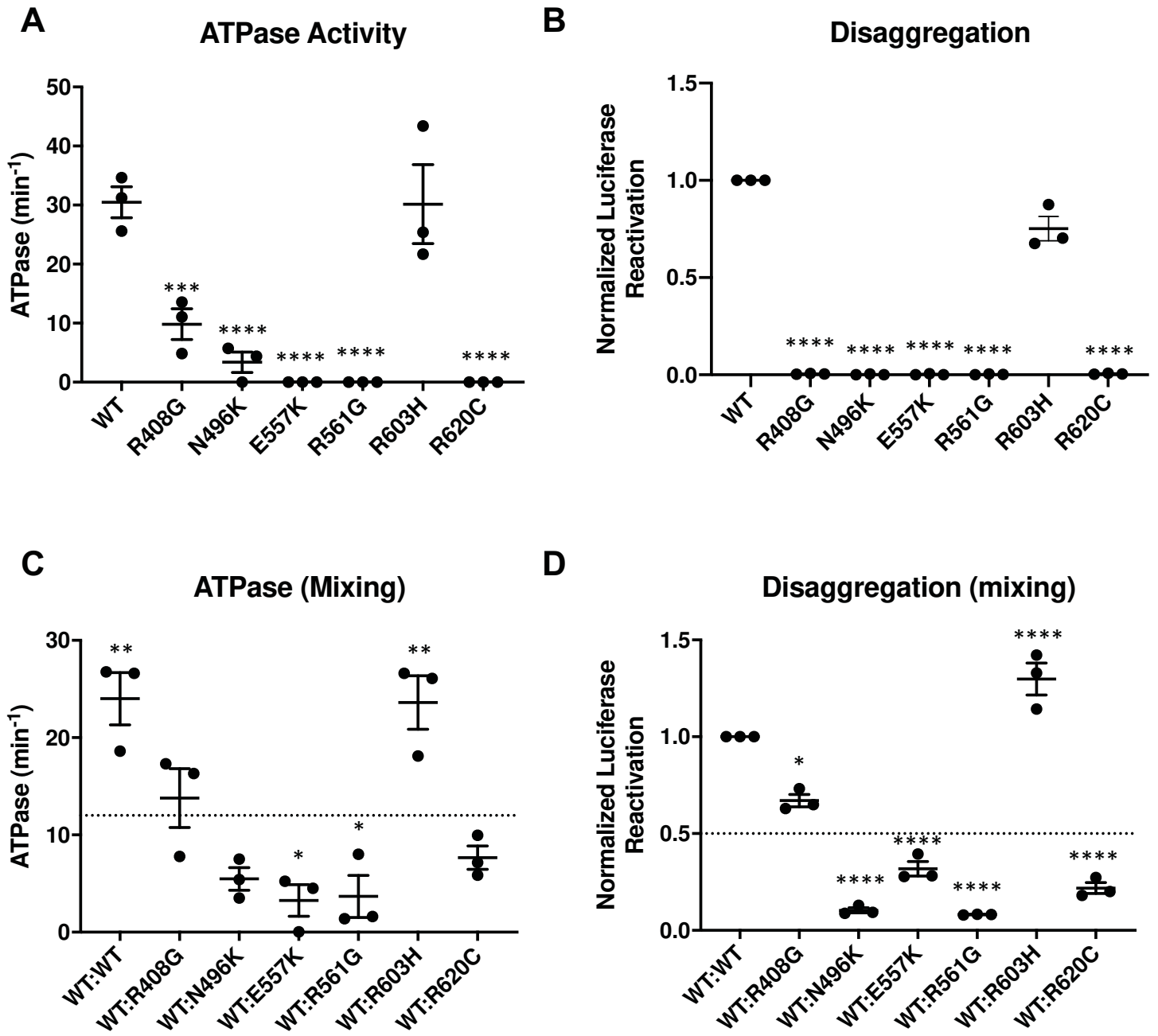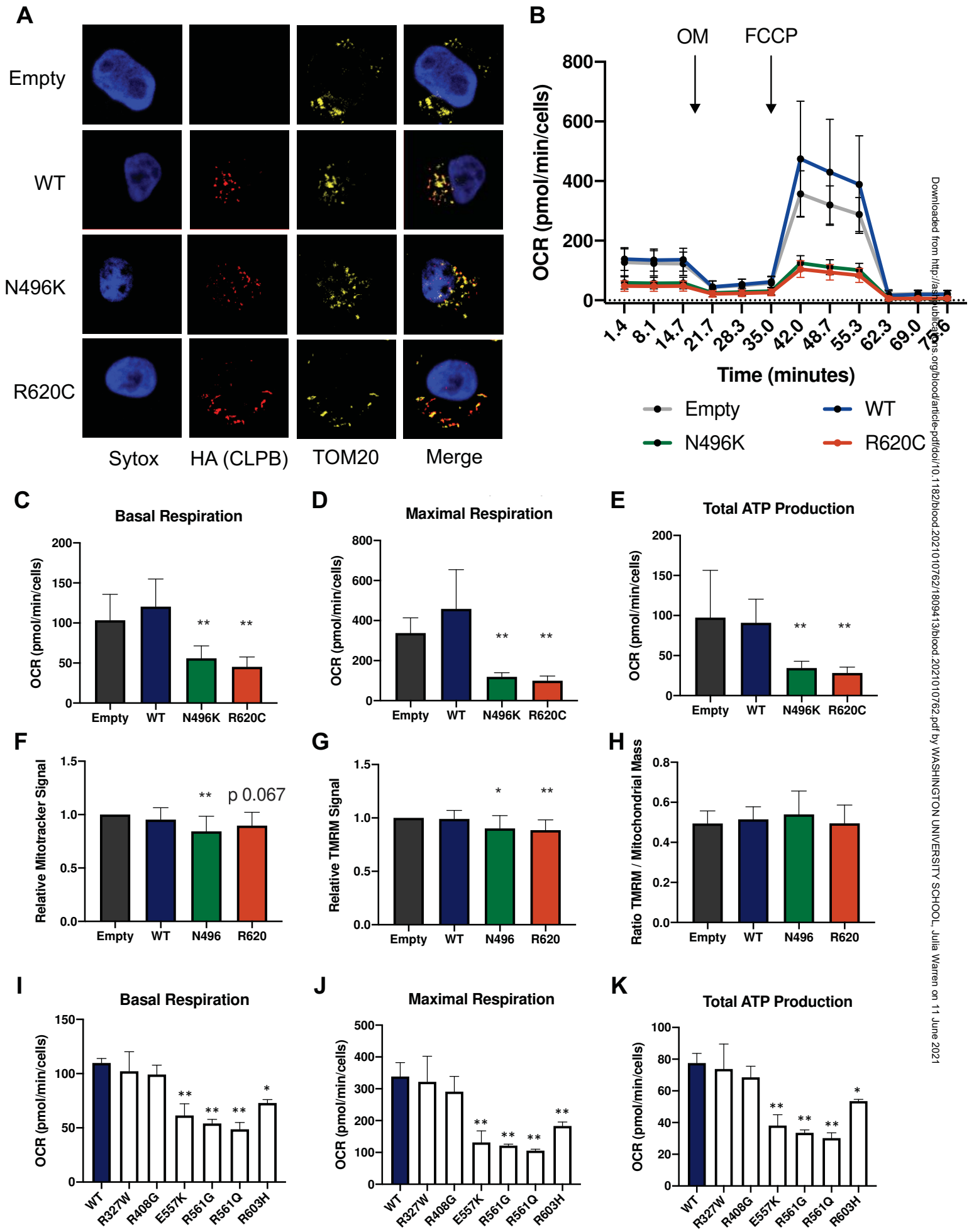
Figure 1

Figure 2

Figure 3

Figure 4

Figure 5

Figure 6

A

HSPA5

B

Caspase3+

C

Annexin V+

D

Caspase3+ fold-change

E

Annexin V+